



*Supplement of*

## **Receptor modelling of fine particles in southern England using CMB including comparison with AMS-PMF factors**

J. Yin et al.

*Correspondence to:* R. M. Harrison ([r.m.harrison@bham.ac.uk](mailto:r.m.harrison@bham.ac.uk))

**Table S1.** List of all organic markers analysed

<i>n-Alkanes</i>	Abbreviation	<i>Hopanes</i>	Abbreviation	<i>PAHs</i>	Abbreviation
<i>n</i> -Tetracosane	C24	17 $\alpha$ (H)-22,29,30-Trisnorhopane	17 $\alpha$ TNohop	Benzo[k]fluoranthene	B[k]F
<i>n</i> -Pentacosane	C25	17 $\alpha$ (H),21 $\beta$ (H)-Hopane	17 $\alpha\beta$ Hop	Benzo[b]fluoranthene	B[b]F
<i>n</i> -Hexacosane	C26	17 $\beta$ (H),21 $\alpha$ (H)-30-norhopane	17 $\beta\alpha$ Nohop	Benzo[e]pyrene	B[e]P
<i>n</i> -Heptacosane	C27	22S-17 $\alpha$ (H),21 $\beta$ (H)-30-Homohopane	22S $\alpha\beta$ HH	Benzo[a]pyrene	B[a]P
<i>n</i> -Octacosane	C28	22R-17 $\alpha$ (H),21 $\beta$ (H)-30-Homohopane	22R $\alpha\beta$ HH	Perylene	PER
<i>n</i> -Nonacosane	C29	22S-17 $\alpha$ (H),21 $\beta$ (H)-30-Bishomohopane	22S $\alpha\beta$ BHH	Indeno[1,2,3-cd]pyrene	IP
<i>n</i> -Triacontane	C30	22R-17 $\alpha$ (H),21 $\beta$ (H)-30-Bishomohopane	22R $\alpha\beta$ BHH	Dibenz[a,h]anthracene	D[ah]A
<i>n</i> -Hentriacontane	C31	22S-17 $\alpha$ (H),21 $\beta$ (H)-30,31,32-trishomohopane	22S $\alpha\beta$ THH	Benzo[ghi]perylene	B[ghi]PER
<i>n</i> -Dotriacontane	C32	22R-17 $\alpha$ (H),21 $\beta$ (H)-30,31,32-trishomohopane	22R $\alpha\beta$ THH	Coronene	COR
<i>n</i> -Tritriacontane	C33	<b>Fatty acids</b>		Picene	PIC
<i>n</i> -Tetracontane	C34	Tetradecanoic acid/Myristic acid (C14)	MyrA	<b>Secondary markers</b>	
<i>n</i> -Pentacontane	C35	Pentadecanoic acid/Pentadecyllic acid (C15)	PentA	Pinonic acid	PinoA
<b>Sterols</b>		Hexadecanoic acid/Palmitic acid (C16)	PalmA	Pinic acid	PinicA
Levoglucosan	Levo	Octadecanoic acid/Stearic acid (C18)	SteaA	2-methylthreitol	MethT
Cholesterol	Chol	9-octadecenoic acid/Oleic acid (C18:1)	OleiA	2-methylerythritol	MethE
		9,12-octadecadienoic acid/Linoleic acid (C18:2)	LinoA		

**Table S2. Precision (%) and method detection limit (MDL)(ng m<sup>-3</sup>) for the target compounds**

<b><i>n-Alkanes</i></b>	Precision	MDL	<b><i>Hopanes</i></b>	Precision	MDL	<b><i>PAHs</i></b>	Precision	MDL
C24	5.1	0.027	17aTNohop	4.7	0.010	B[b]F	6.2	0.015
C25	4.4	0.041	17abNohop	5.1	0.011	B[k]F	4.3	0.017
C26	7.1	0.055	17baNohop	3.4	0.017	B[e]P	5.3	0.019
C27	5.7	0.026	17abHop	5.5	0.014	B[a]P	4.9	0.014
C28	10.8	0.019	22SabHH	4.3	0.015	PER	5.8	0.010
C29	13.4	0.048	22RabHH	4.4	0.018	IP	8.9	0.008
C30	10.7	0.066	22SabBHH	5.1	0.016	D[ah]A	6.6	0.011
C31	8.1	0.034	22RabBHH	5.7	0.047	PIC	15.0	0.025
C32	8.8	0.044	22SabTHH	5.2	0.014	B[ghi]PER	7.5	0.017
C33	15.9	0.034	22RabTHH	6.3	0.035	COR	3.2	0.016
C34	3.3	0.015	<b><i>Fatty acids</i></b>					
C35	7.5	0.054	MA	11.9	0.57			
<b><i>Sterols</i></b>			PentA	8.8	0.23	<b><i>Secondary Markers</i></b>		
Levo	15.4	0.23	PA	20.4	2.1	PinoA	15.7	0.37
Chol	5.6	0.024	LOA	6.8	0.097	PinicA	8.1	0.19
			OA	9.2	0.31	MethT	5.9	0.035
			SA	19.2	1.3	MethE	7.4	0.10

**Table S3. Dependence of mean mass of PMF factors upon value of fpeak=0**

Factor fPeak value \	OOA Mean mass	SFOA1 Mean mass	SFOA2 Mean mass	COA Mean mass	HOA Mean mass
-0.6	0.897374	0.757835	0.882626	1.02376	0.68164
0	0.933063	0.747544	0.857564	0.875335	0.829156
1	0.940803	0.696752	0.776001	0.682512	1.14724

**Table S4: Source contribution estimates (SCE) ( $\mu\text{g m}^{-3}$ ) and standard deviation (S.D.) for fine particulate OC and PM<sub>2.5</sub> at NK and HAR from the CMB model (averaged from daily CMB outputs)**

<i>Source Name</i>	SCE	OC		PM <sub>2.5</sub>		OC/PM <sub>2.5</sub> or OC/OM CF <sup>c</sup>		
		NK <sup>a</sup>	NK <sup>b</sup>	HAR <sup>a</sup>	NK <sup>a</sup>	NK <sup>b</sup>	HAR <sup>a</sup>	
<i>Vegetation</i>	SCE	0.069	0.069	0.11	0.21	0.21	0.35	0.324
	S.D.	0.010	0.010	0.015	0.030	0.030	0.048	-
<i>Woodsmoke</i>	SCE	0.53	0.53	0.64	0.64	0.64	0.77	0.836
	S.D.	0.11	0.11	0.14	0.14	0.14	0.16	-
<i>Natural Gas</i>	SCE	0.046	0.046	0.042	0.054	0.054	0.050	0.849
	S.D.	0.009	0.009	0.007	0.011	0.011	0.008	-
<i>Dust/Soil</i>	SCE	0.049	0.049	<b>0.018</b>	0.38	0.38	<b>0.14</b>	0.131
	S.D.	0.037	0.037	0.015	0.29	0.29	0.11	0.0133
<i>Coal</i>	SCE	0.075	0.075	0.041	0.17	0.17	0.094	0.432
	S.D.	0.020	0.020	0.009	0.046	0.046	0.021	0.0834
<i>Food Cooking</i>	SCE	0.32	0.32	0.070	0.56	0.56	0.12	0.566
	S.D.	0.055	0.055	0.013	0.10	0.10	0.023	0.030
<i>Total Traffic</i>	SCE	0.81	0.81	0.35	1.40	1.40	0.59	0.579
	S.D.	0.39	0.39	0.16	0.88	0.88	0.29	0.051
<i>Biogenic Secondary</i>	SCE	-	0.90	-	-	1.63	-	0.556
	S.D.	-	0.17	-	-	0.31	-	-
<i>Other OC/OM</i>	SCE	1.62	0.72	1.03	2.92	1.29	1.85	0.556
	S.D.	-	-	-	-	-	-	-
<i>Sea Salt</i>	SCE	-	-	-	1.1	1.1	0.82	-
	S.D.	-	-	-	0.020	0.020	0.020	-
<i>Ammonium Sulphate</i>	SCE	-	-	-	2.2	2.2	2.1	-
	S.D.	-	-	-	0.028	0.028	0.028	-
<i>Ammonium Nitrate</i>	SCE	-	-	-	5.8	5.8	4.1	-
	S.D.	-	-	-	0.072	0.072	0.072	-
<i>Measured OC/PM<sub>2.5</sub></i>	Mass	3.5	3.5	2.3	15.7	15.7	11.0	-

Note: Figures in bold were not statistically different from zero; *a* - Modelled without biogenic secondary source profile; *b* – Modelled with biogenic secondary source profile; *c* – Conversion factor

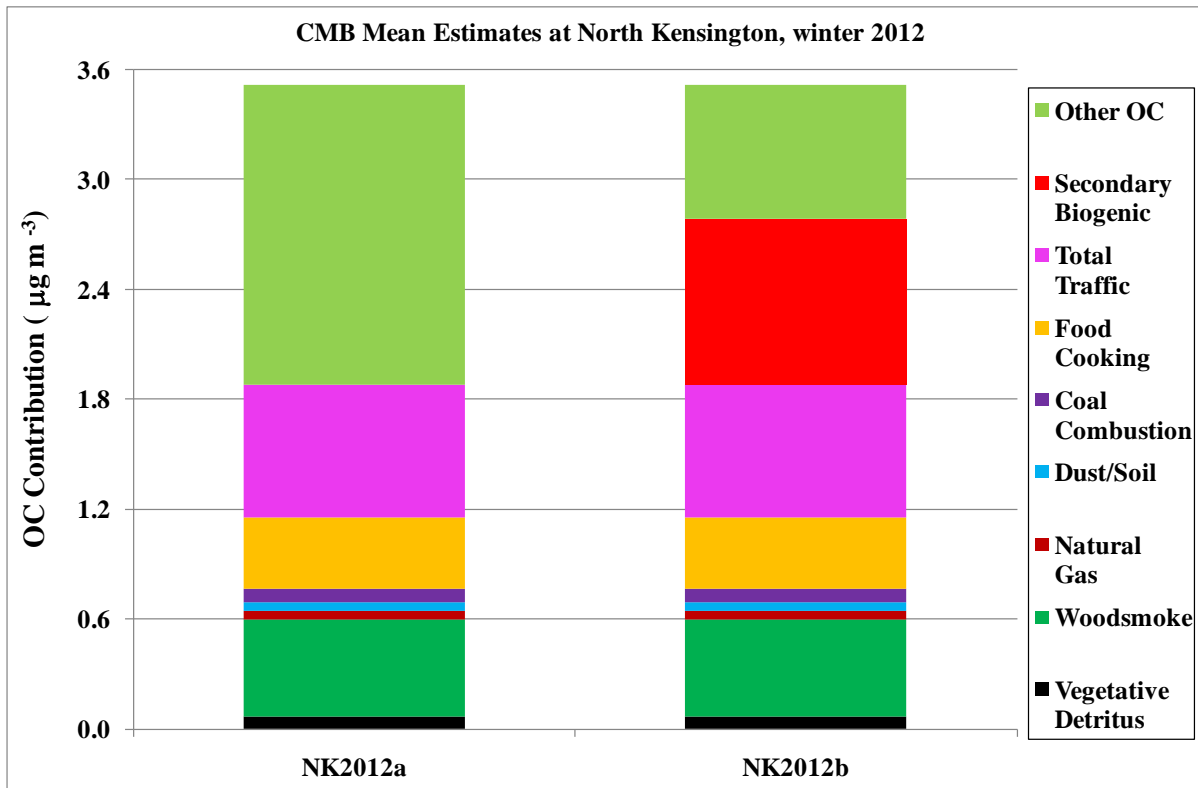
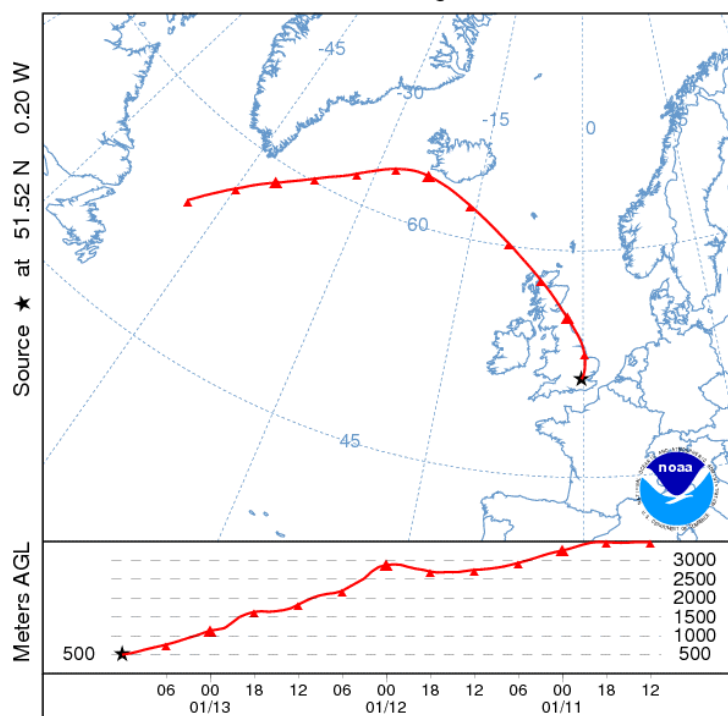
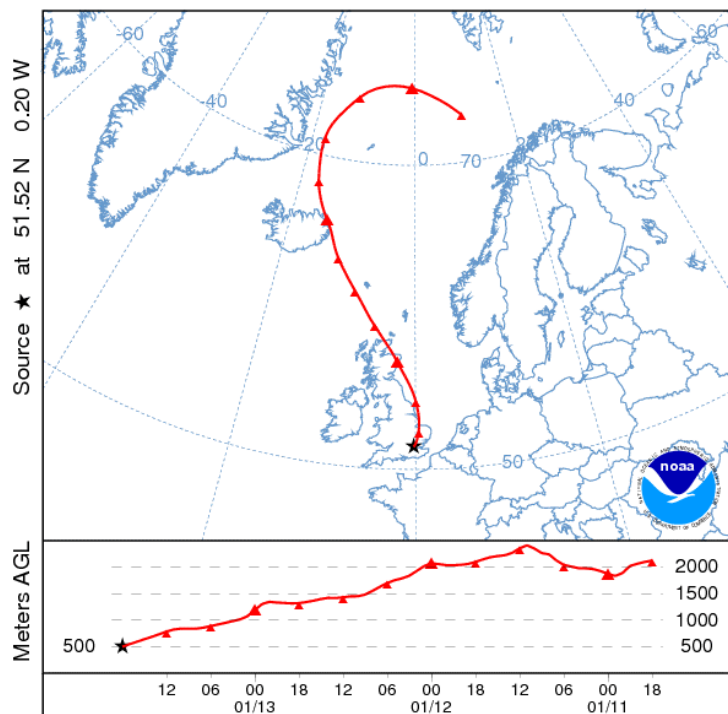


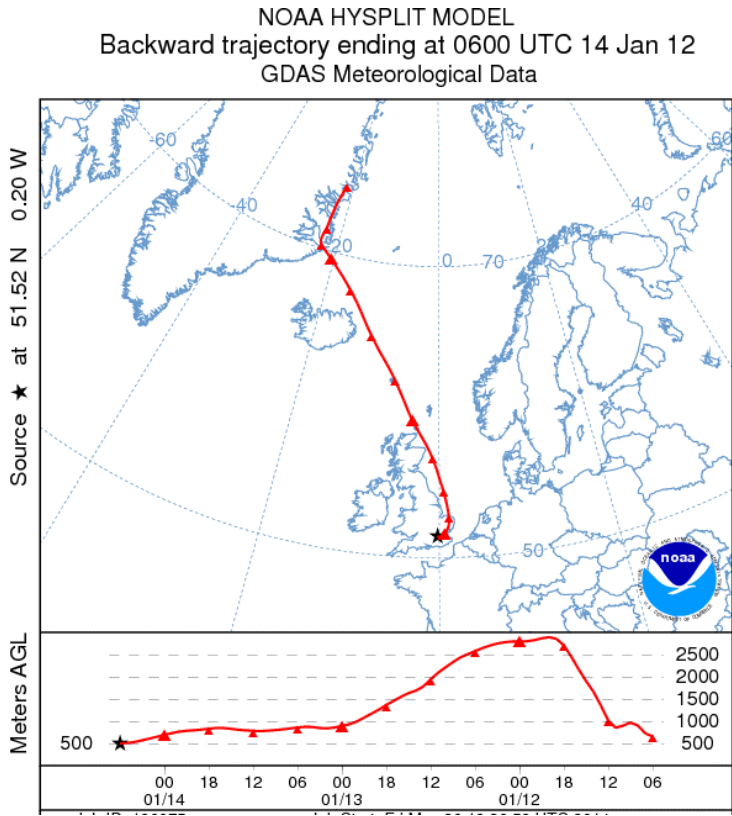
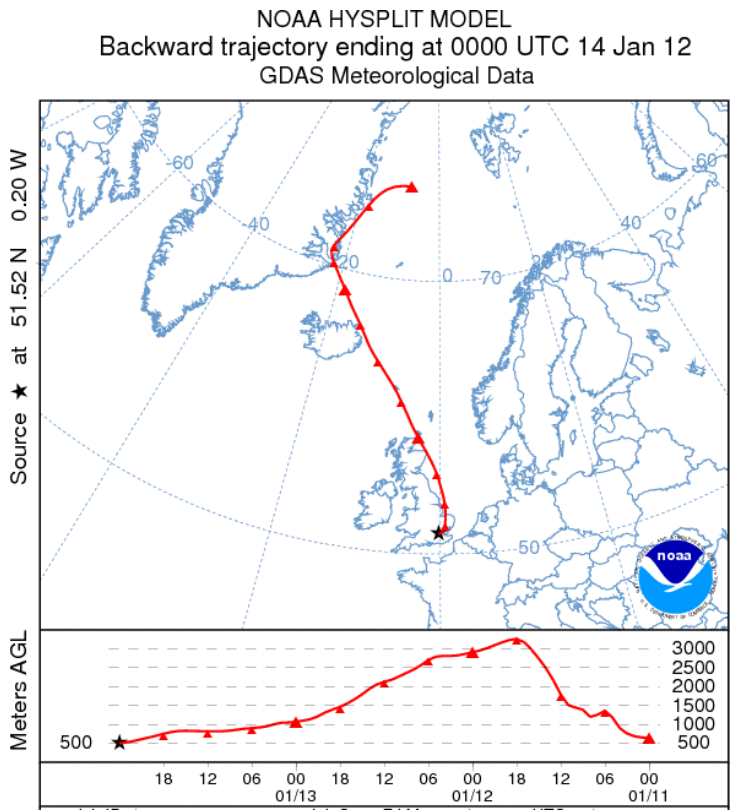
**Figure S1:** Mean OC source contribution estimates with (b) and without (a) secondary biogenic component at NK

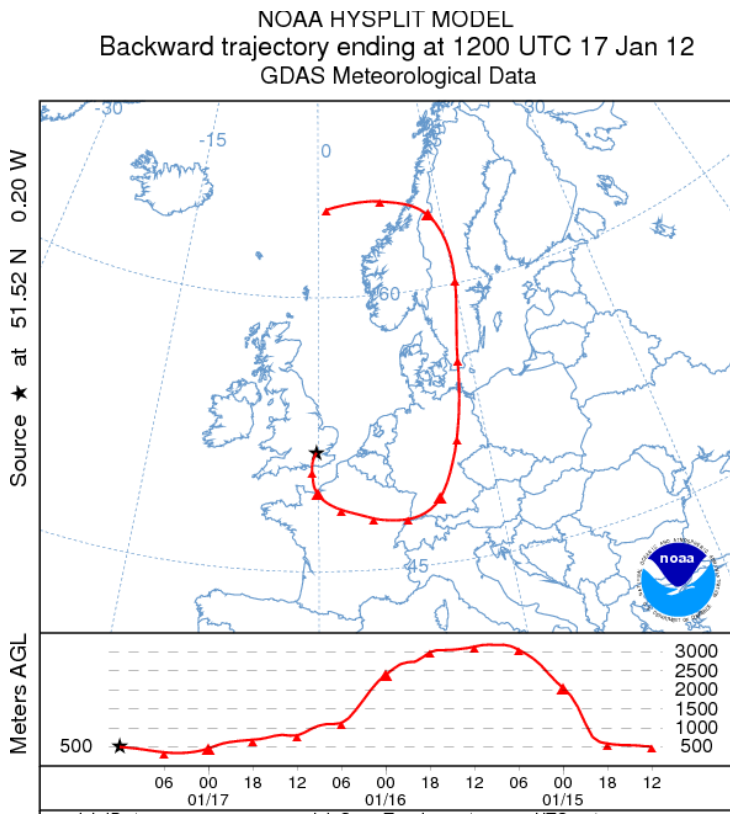
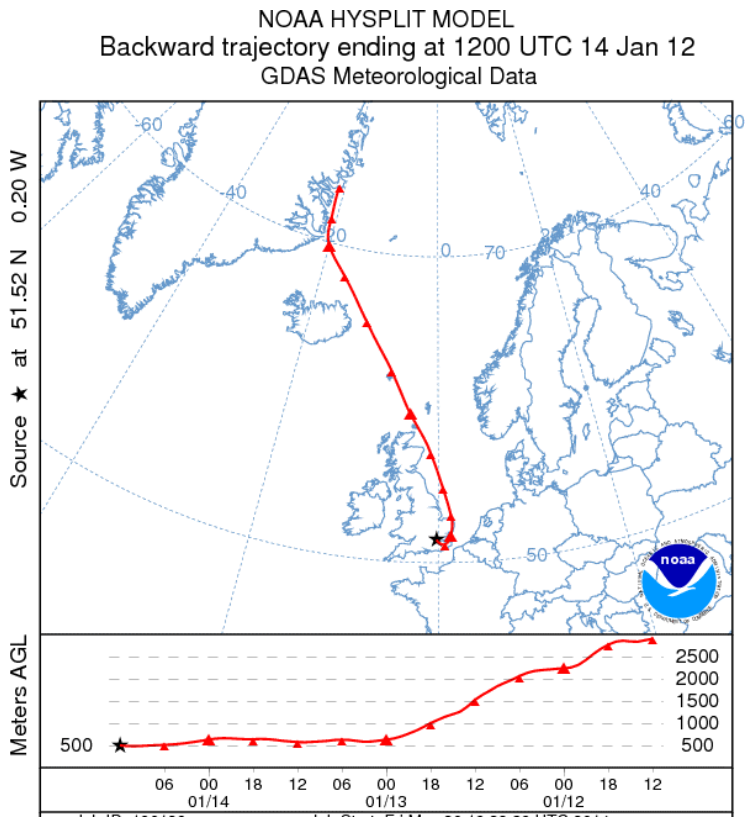
NOAA HYSPLIT MODEL  
Backward trajectory ending at 1200 UTC 13 Jan 12  
GDAS Meteorological Data



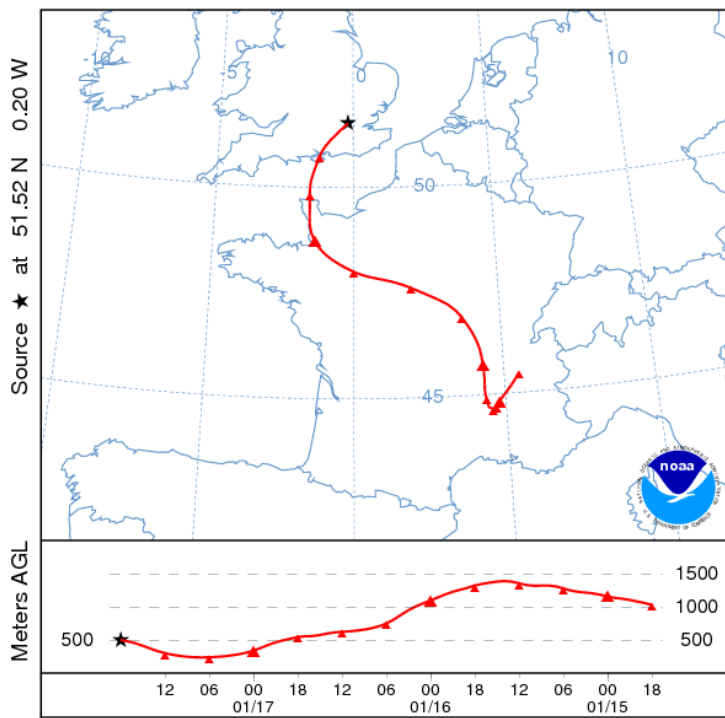
NOAA HYSPLIT MODEL  
Backward trajectory ending at 1800 UTC 13 Jan 12  
GDAS Meteorological Data



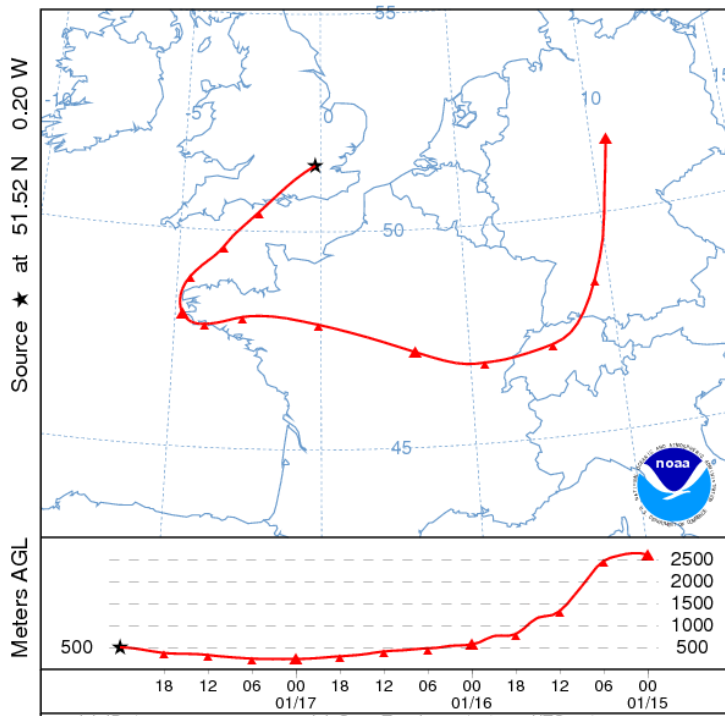




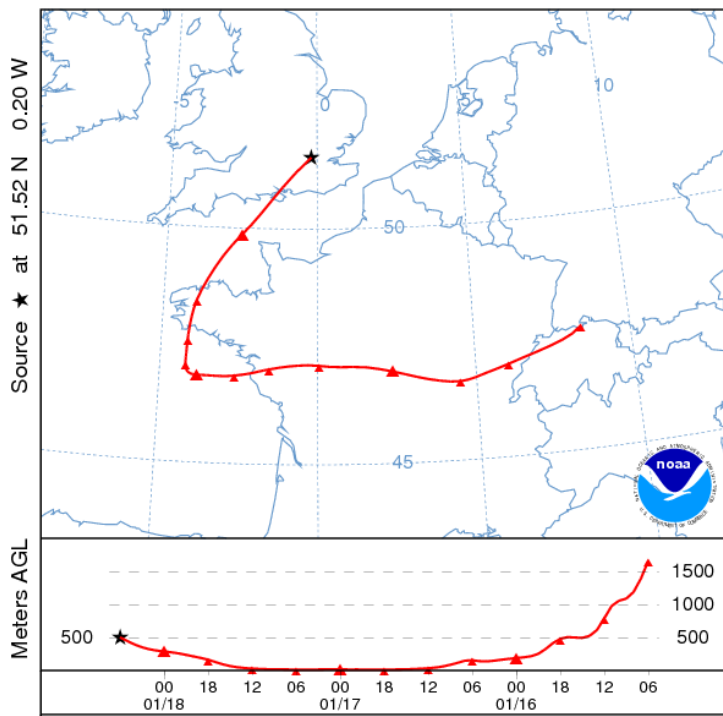
NOAA HYSPLIT MODEL  
Backward trajectory ending at 1800 UTC 17 Jan 12  
GDAS Meteorological Data



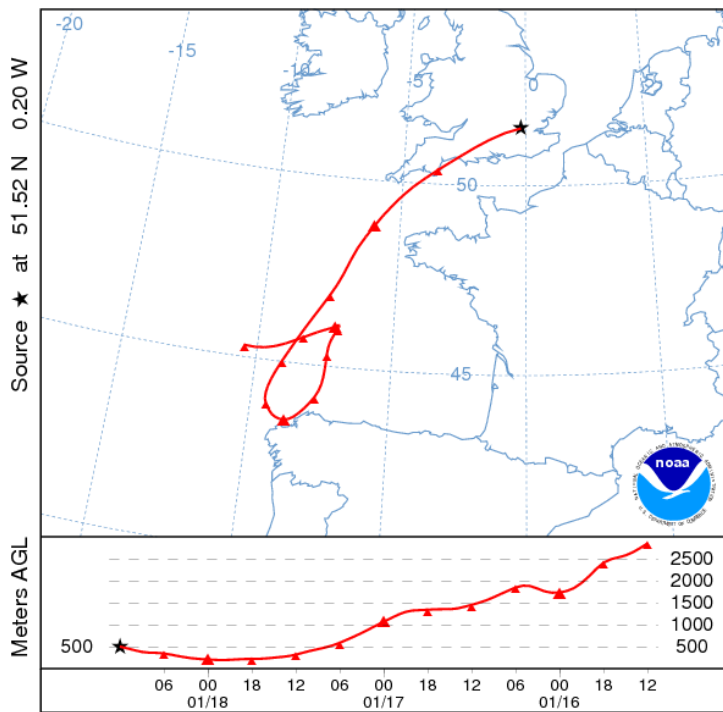
NOAA HYSPLIT MODEL  
Backward trajectory ending at 0000 UTC 18 Jan 12  
GDAS Meteorological Data

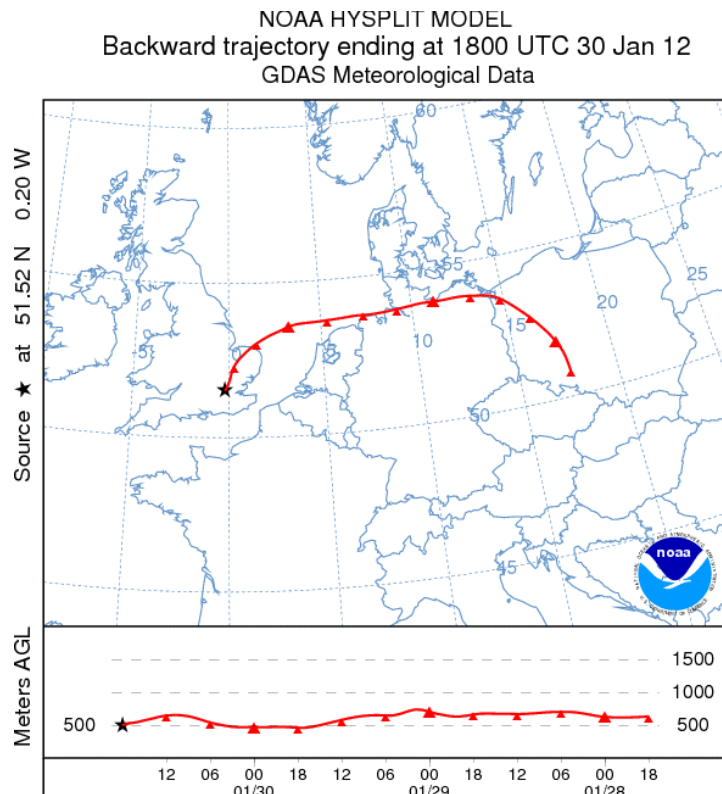
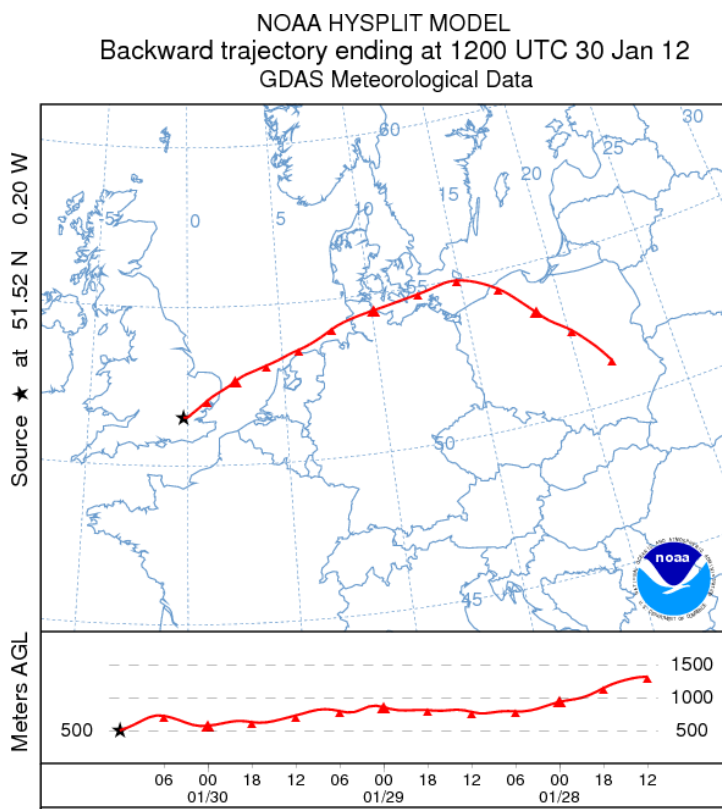


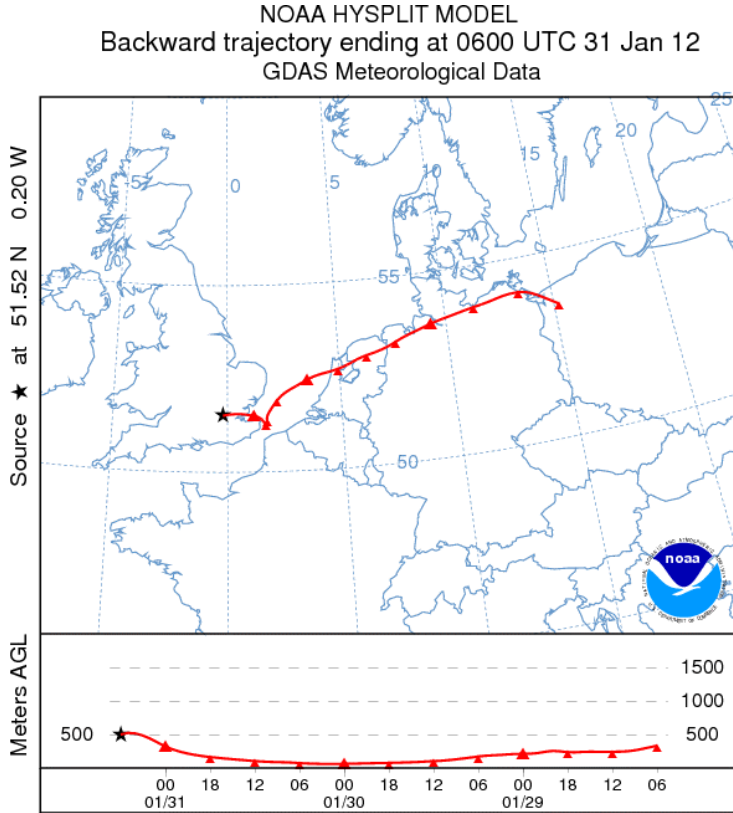
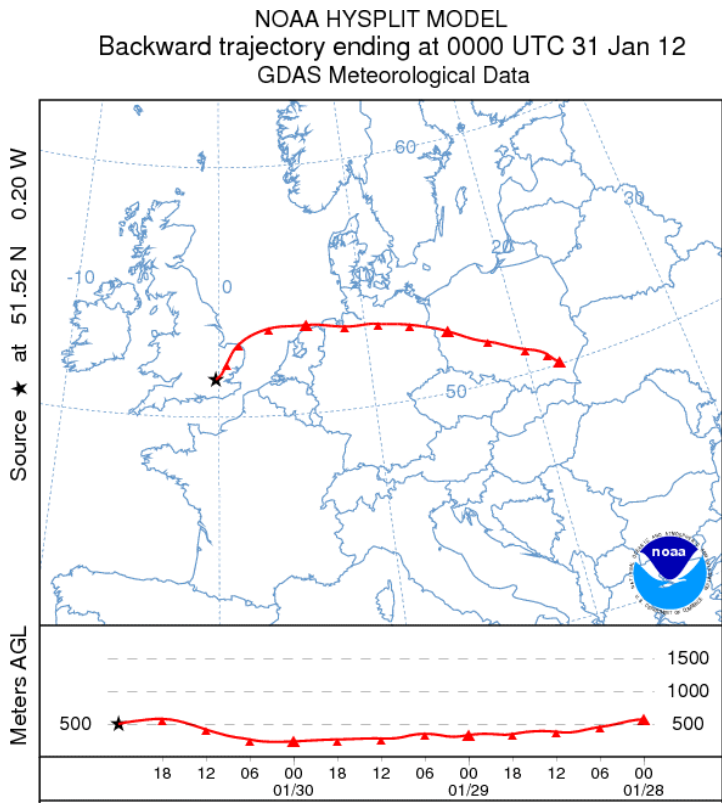
NOAA HYSPLIT MODEL  
Backward trajectory ending at 0600 UTC 18 Jan 12  
GDAS Meteorological Data



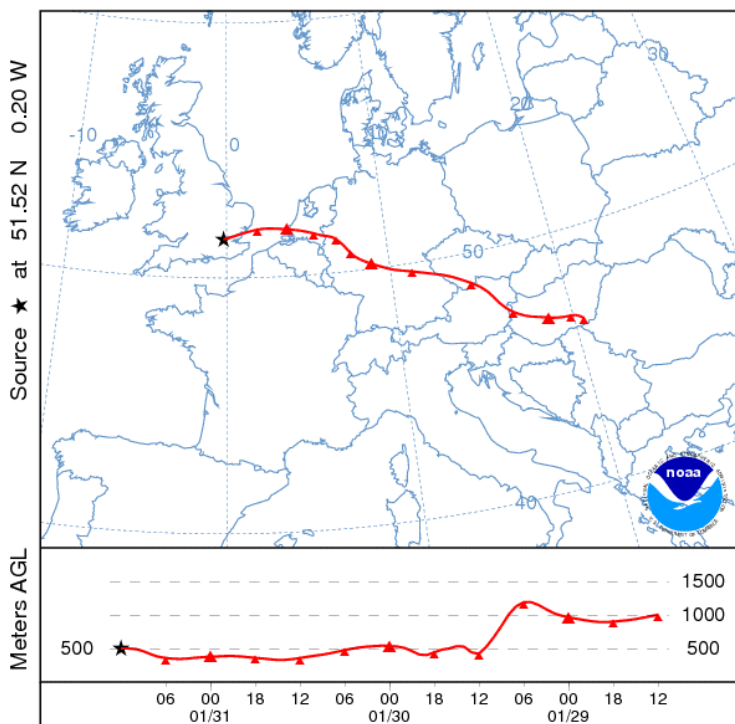
NOAA HYSPLIT MODEL  
Backward trajectory ending at 1200 UTC 18 Jan 12  
GDAS Meteorological Data



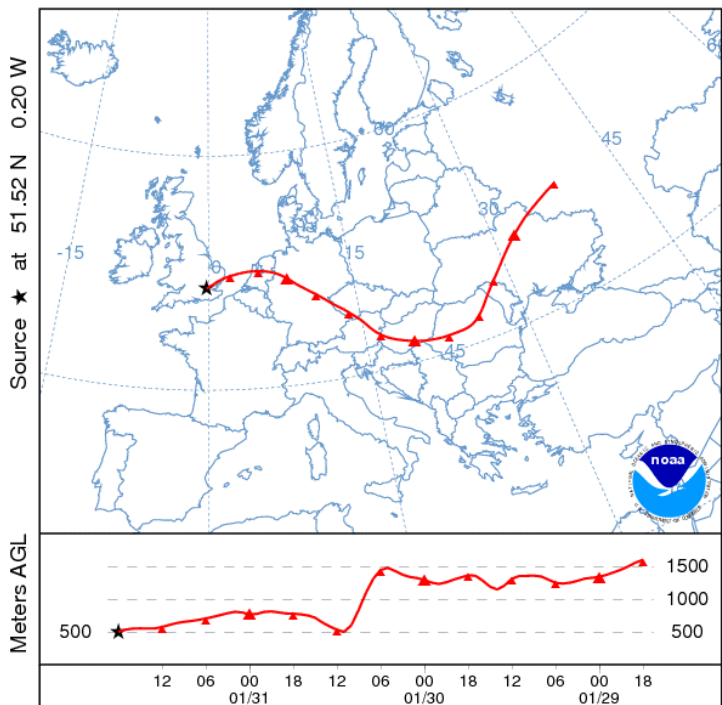


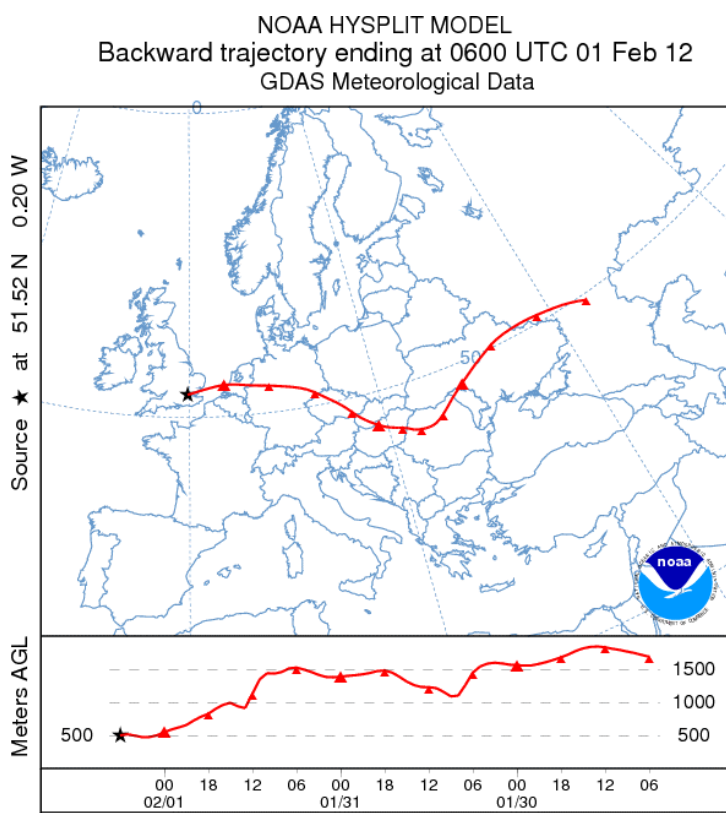
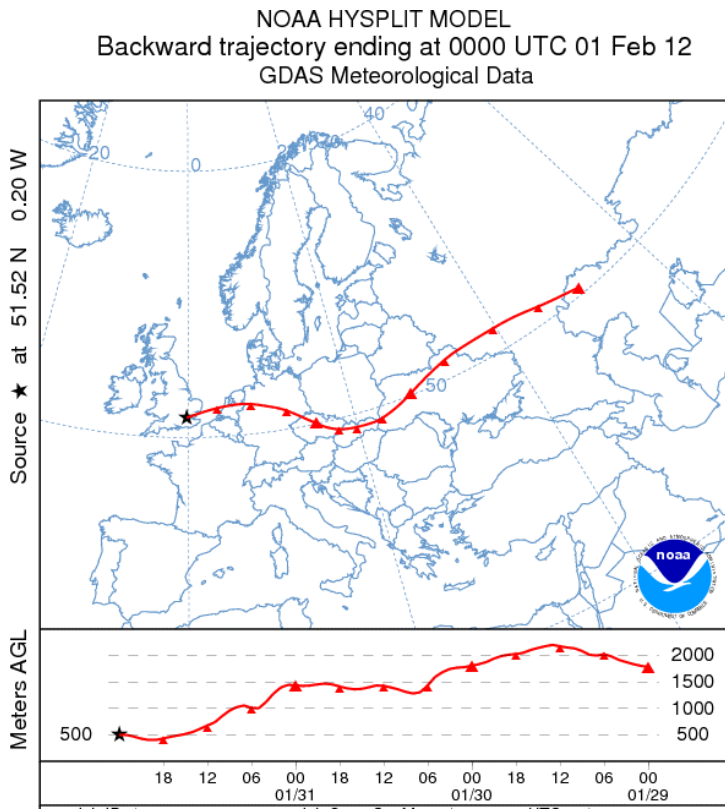


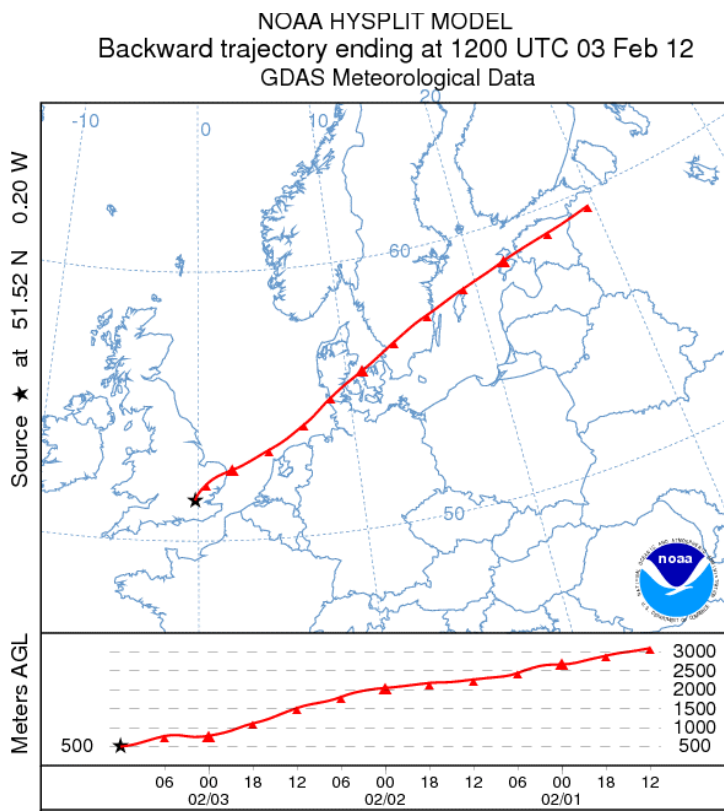
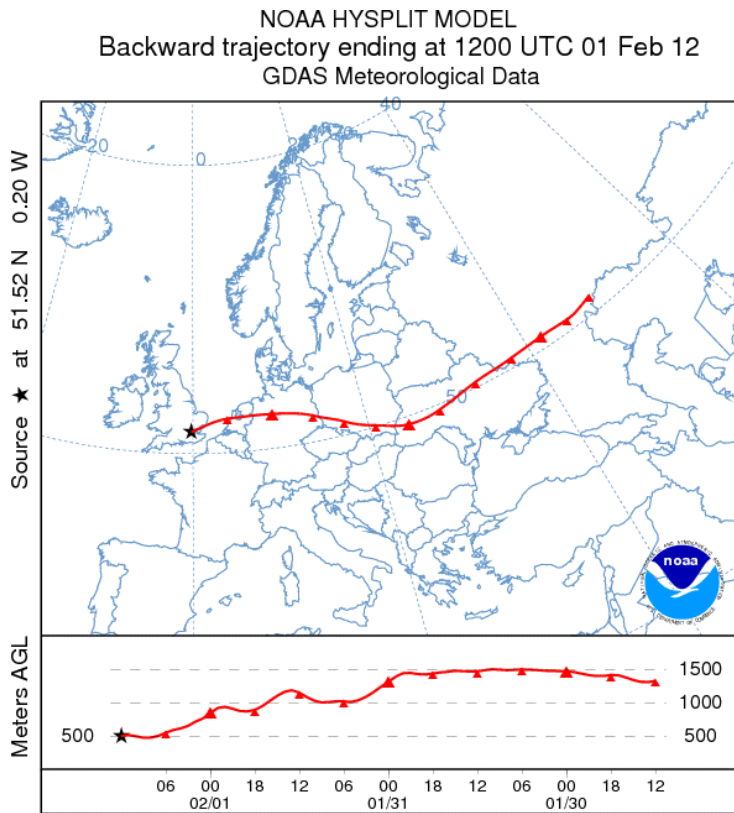
NOAA HYSPLIT MODEL  
Backward trajectory ending at 1200 UTC 31 Jan 12  
GDAS Meteorological Data



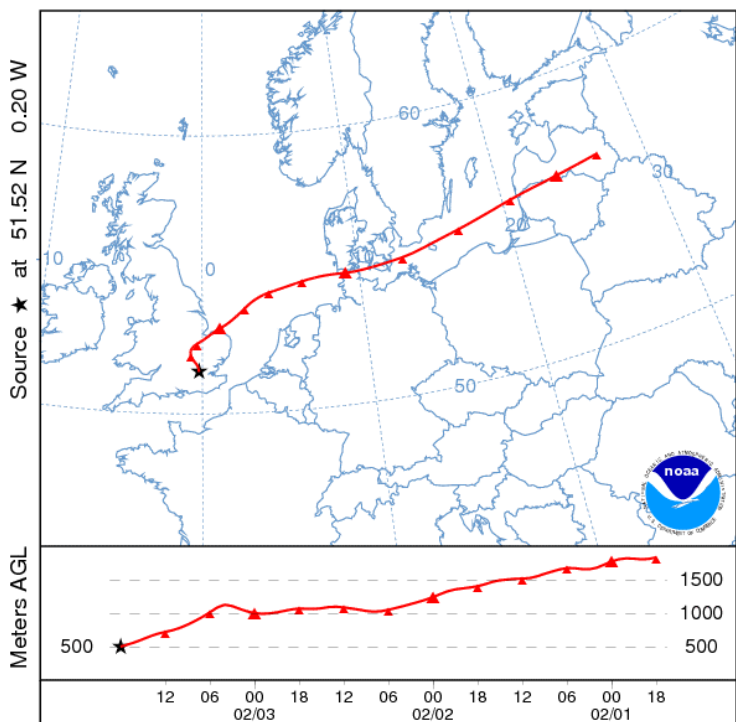
NOAA HYSPLIT MODEL  
Backward trajectory ending at 1800 UTC 31 Jan 12  
GDAS Meteorological Data



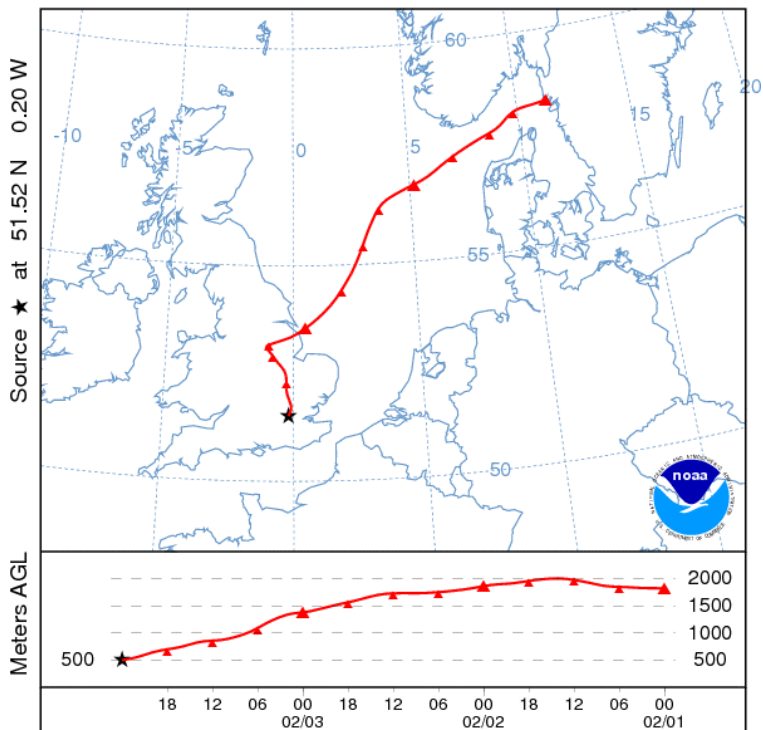




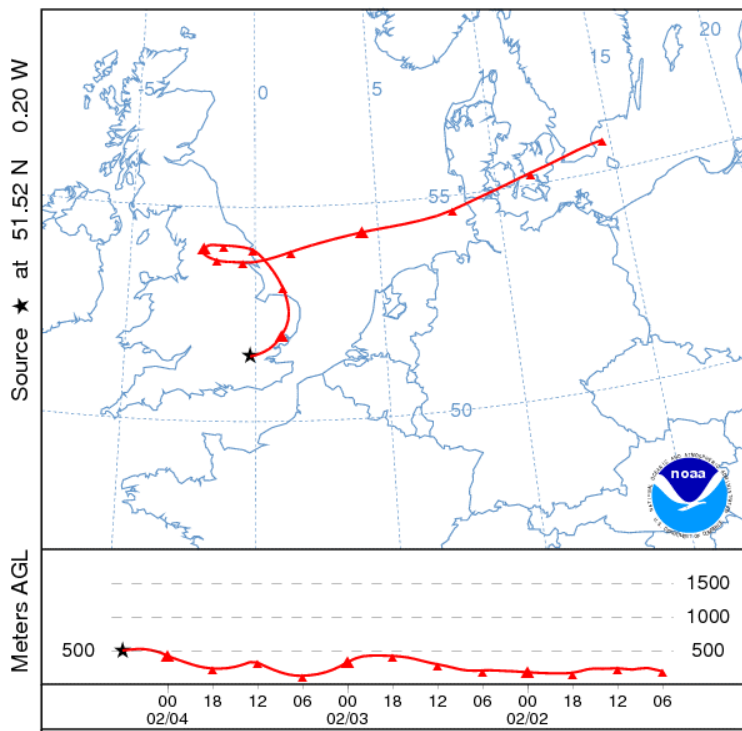
NOAA HYSPLIT MODEL  
Backward trajectory ending at 1800 UTC 03 Feb 12  
GDAS Meteorological Data



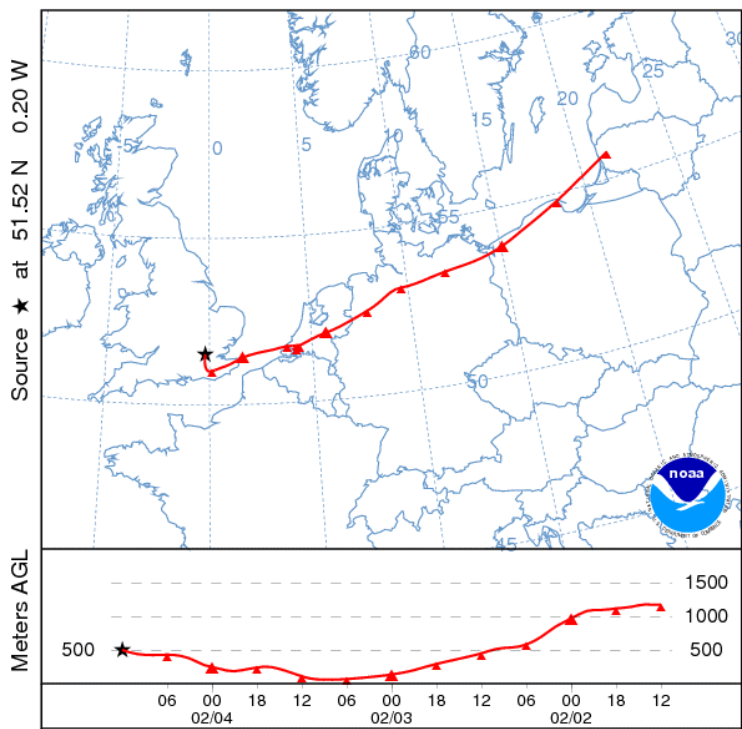
NOAA HYSPLIT MODEL  
Backward trajectory ending at 0000 UTC 04 Feb 12  
GDAS Meteorological Data



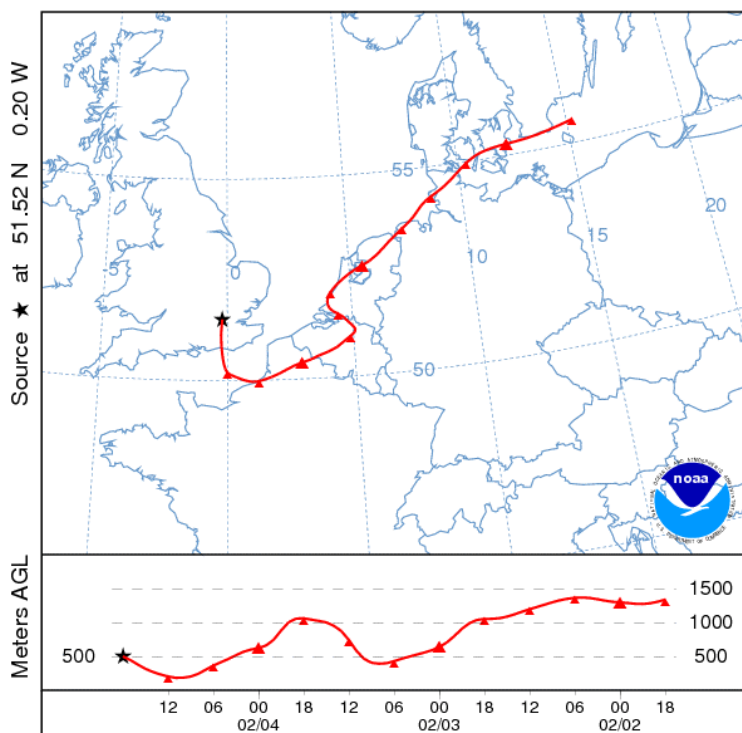
NOAA HYSPLIT MODEL  
Backward trajectory ending at 0600 UTC 04 Feb 12  
GDAS Meteorological Data



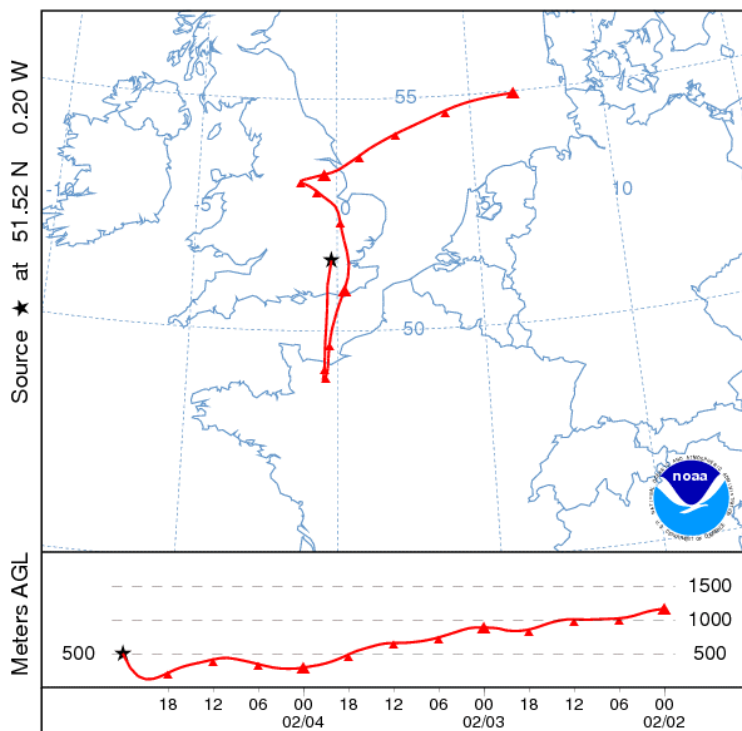
NOAA HYSPLIT MODEL  
Backward trajectory ending at 1200 UTC 04 Feb 12  
GDAS Meteorological Data



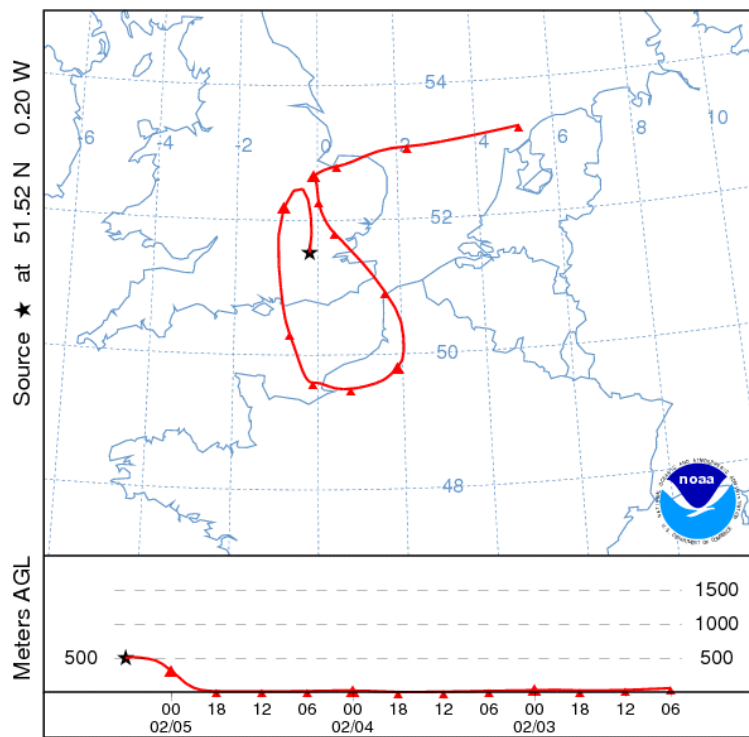
NOAA HYSPLIT MODEL  
Backward trajectory ending at 1800 UTC 04 Feb 12  
GDAS Meteorological Data



NOAA HYSPLIT MODEL  
Backward trajectory ending at 0000 UTC 05 Feb 12  
GDAS Meteorological Data



NOAA HYSPLIT MODEL  
 Backward trajectory ending at 0600 UTC 05 Feb 12  
 GDAS Meteorological Data



NOAA HYSPLIT MODEL  
 Backward trajectory ending at 1200 UTC 05 Feb 12  
 GDAS Meteorological Data

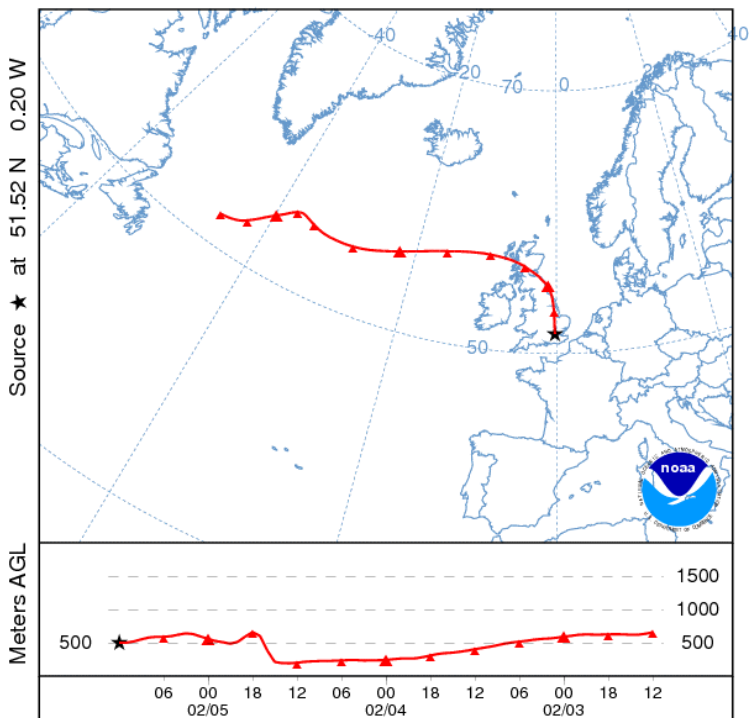


**Figure S2.** Air mass back trajectories at NK for starting dates of January 13<sup>th</sup>, 17<sup>th</sup>, 30<sup>th</sup>, 31<sup>st</sup> and February 3<sup>rd</sup>, 4<sup>th</sup>.